0026-895X/03/6303-547–556$7.00
MOLECULAR PHARMACOLOGY
Copyright © 2003 The American Society for Pharmacology and Experimental Therapeutics
Mol Pharmacol 63:547–556, 2003

Vol. 63, No. 3
1894/1049867
Printed in U.S.A.

Molecular Site of Action of the Antiarrhythmic Drug Propafenone at the Voltage-Operated Potassium Channel Kv2.1

MICHAEL MADEJA, THORSTEN LEICHER, PATRICK FRIEDERICH, MARK A. PUNKE, WILHELM HAVERKAMP, ULRICH MUßHOFF, GÜNTER BREITHARDT, ERWIN-JOSEF SPECKMANN

Institute of Physiology (M.M., U.M., E.-J.S.) and Department of Cardiology and Angiology (W.H., G.B.), University of Münster, Münster, Germany; Hertie Foundation, Department of Neuroscience/Multiple Sclerosis, Frankfurt, Germany (M.M.); Center of Molecular Neurobiology, University of Hamburg, Hamburg, Germany (T.L.); and Department of Anesthesiology, University Hospital Hamburg, Hamburg, Germany (P.F., M.A.P.)

Received June 4, 2002; accepted December 2, 2002

This article is available online at http://molpharm.aspetjournals.org

ABSTRACT

The effects of the antiarrhythmic drug propafenone at Kv2.1 channels were studied with wild-type and mutated channels expressed in *Xenopus laevis* oocytes. Propafenone decreased the Kv2.1 currents in a time- and voltage-dependent manner (decrease of the time constants of current rise, increase of block with the duration of voltage steps starting from a block of less than 19%, increase of block with the amplitude of depolarization yielding a fractional electrical distance δ of 0.11 to 0.16). Block of Kv2.1 appeared with application to the intracellular, but not the extracellular, side of membrane patches. In mutagenesis experiments, all parts of the Kv2.1 channel were successively exchanged with those of the Kv1.2 channel, which is much more sensitive to propafenone. The intracellular amino and carboxyl terminus and the intracellular linker S4-S5 reduced the blocking effect of propafenone, whereas the linker S5-S6, as well as the segment S6 of the Kv1.2 channel, abolished it to the value of the Kv1.2 channel. In the linker S5-S6, this effect could be narrowed down to two groups of amino acids (groups 372 to 374 and 383 to 384), which also affected the sensitivity to tetraethylammonium. In segment S6, several amino acids in the intracellularly directed part of the helix significantly reduced propafenone sensitivity. The results suggest that propafenone blocks the Kv2.1 channel in the open state from the intracellular side by entering the inner vestibule of the channel. These results are consistent with a direct interaction of propafenone with the lower part of the pore helix and/or residues of segment S6.

Voltage-operated potassium currents play important roles in shaping and terminating cardiac action potentials. Although several potassium current components have been isolated, two types of currents can be distinguished: fast activating and inactivating currents, referred to as I_{to}, and delayed, more slowly inactivating currents, referred to as I_K (Snyders, 1999). The molecular correlates underlying these current components, however, have not yet been clearly determined. For I_K, in particular, several candidates have been identified or discussed. The mRNA of the potassium channel families Kv1, Kv2, Kv3, and Kv4 are present in significant amounts in cardiomyocytes (Dixon and McKinnon, 1994; Barry et al., 1995; Brahmajothi et al., 1996) and, after expression in heterologous systems, yield currents sharing functional characteristics with native I_K (Snyders, 1999). Much attention has been focused on the Kv1.5 potassium channel, which is assumed to be the molecular correlate of the very rapidly activating subcomponent of I_K, referred to as I_{Kur} (Snyders, 1999).

Another possible molecular correlate for I_K, however, might be Kv2.1. Cardiomyocytes of transgenic mice expressing dominant negative Kv2.1 subunits showed a reduction of I_K and a marked prolongation of action potentials (Xu et al., 1999). Accordingly, spontaneously triggered activity was found in some myocytes of these transgenic mice. This correlated with the observation that Kv2.1 mRNA is only present in part of wild-type myocytes (Brahmajothi et al., 1996; Schultz et al., 2001). The expression of Kv2.1 channels in heart is altered under pathologic conditions associated with arrhythmias. Thus, 1) hyperthyroidism drastically decreased the mRNA level of Kv2.1 in rat ventricular myocytes (Nishiyama et al., 1998), 2) rats with infracted myocardium showed increased action potential durations and reduced protein levels of Kv2.1 (Huang et al., 2000), 3) cardiac hyper-

This study was supported by Deutsche Forschungsgemeinschaft grant SFB 556/A3.

ABBREVIATIONS: PROP, propafenone; nt, nucleotide; CHO, Chinese hamster ovary; TEA, tetraethylammonium chloride; HERG, human *ether-a-go-go*-related gene; MK-499, (+)-*N*-[1′-(6-cyano-1,2,3,4-tetrahydro-2(*R*)-naphthalenyl)-3,4-dihydro-4(*R*)-hydroxyspiro(2*H*-1-benzopyran-2,4′-piperidin)-6-yl]methanesulfonamide] monohydrochloride.

trophy in rats (induced by phorbol esters) increased the density of Kv2.1 (Walsh et al., 2001), and 4) diabetic cardiomyopathy (induced by streptozotocin) yielded a decrease of Kv2.1 protein density in rat left ventricular myocytes (Qin et al., 2001).

Several drugs have been developed to prevent arrhythmias (Singh, 1997). A widely used substance is 2′-[3′(propylamino)-2-(hydroxy)propoxy]-3-phenylpropiophenone hydrochloride; [propafenone (PROP)]. Electrophysiological studies using animal models have shown that PROP reduces the maximum rate of rise and the amplitude of the action potential (Ledda et al., 1981). Accordingly, sodium channel blocking effects of PROP were described previously (Kohlhardt, 1984). Also, PROP increased the duration of the action potential (Satoh and Hashimoto, 1984; Delgado et al., 1985) and depressed the transient outward current (I_{to}) in atrial myocytes of the rabbit and ventricular myocytes of the rat (Duan et al., 1993), the hyperpolarization-activated inward current (I_f) in isolated human atrial myocytes (Hoppe and Beuckelmann, 1998), and the delayed rectifier current (I_K) in sinoatrial node cells and atrial myocytes of rabbits and ventricular myocytes of guinea pigs (Satoh and Hashimoto, 1984; Duan et al., 1993). In in vitro expression studies, Kv1.5 and Kv2.1 currents are sensitive to micromolar PROP concentrations (Franqueza et al., 1998; Zhu et al., 1999; Rolf et al., 2000). The sensitivity of Kv2.1 channels to PROP increased 15-fold with coexpression of a Kv6.2 potassium channel subunit (Zhu et al., 1999). Thus, PROP in therapeutic concentrations may significantly affect voltage-operated potassium channels.

In a recent study, we found that among cardiac Kv channels, Kv2.1 channels are particularly sensitive to PROP, whereas Kv1.2 channels are relatively insensitive. To study the molecular site of PROP action at the Kv2.1 channel, we constructed chimeric channels between Kv2.1 and Kv1.2. All constructed chimeras gave functional channels; thus, a systematic exchange of every part of Kv2.1 channel subunits could be performed to identify the PROP site of action. In summary, we found several Kv2.1 channel domains that affect PROP action. The results suggest that PROP binds to the open Kv2.1 channel from the intracellular side. Single-site mutations identified residues of the lower part of the pore helix and the segment S6 most likely to be involved in PROP interaction. The PROP binding site seems to be similar but not identical to the ones reported for other antiarrhythmic agents and potassium channel blockers.

Materials and Methods

In Vitro Mutagenesis and RNA Synthesis. The cDNAs for chimeras between rat Kv1.2 (GenBank accession number X16003) and human Kv2.1 (GenBank accession number X68302) were obtained using an overlap polymerase chain reaction and were cloned into the pGEM vector (Liman et al., 1992). For the chimeras, fragments containing the nucleotides (nt) given below were fused together. The numbers refer to the open reading frame of the respective channel.

Mu1: nt 1–492 of Kv1.2, nt 571-Stop of Kv2.1.
Mu2: nt 1–555 of Kv2.1, nt 478–843 of Kv1.2, nt 862-Stop of Kv2.1.
Mu3: nt 1–882 of Kv2.1, nt 874-1230 of Kv1.2, nt 1240-Stop of Kv2.1.
Mu4: nt 1–1239 of Kv2.1, nt 1231-Stop of Kv1.2.
Mu5: nt 1–882 of Kv2.1, nt 874–936 of Kv1.2, nt 946-Stop of Kv2.1.
Mu6: nt 1–954 of Kv2.1, nt 946–996 of Kv1.2, nt 1006-Stop of Kv2.1.
Mu7: nt 1–1005 of Kv2.1, nt 997-1035 of Kv1.2, nt 1042-Stop of Kv2.1.
Mu8: nt 1–1059 of Kv2.1, nt 1051–1164 of Kv1.2, nt 1171-Stop of Kv2.1.
Mu9: nt 1–1182 of Kv2.1, nt 1174–1230 of Kv1.2, nt 1240-Stop of Kv2.1.
Mu10: nt 1–1059 of Kv2.1, nt 1051–1077 of Kv1.2, nt 1087–1155 of Kv2.1, nt 1147–1164 of Kv1.2, nt 1174-Stop of Kv2.1.
Mu11: nt 1–1095 of Kv2.1, nt 1087–1092 of Kv1.2, nt 1102-Stop of Kv2.1.
Mu12: nt 1–1113 of Kv2.1, nt 1105–1113 of Kv1.2, nt 1123-Stop of Kv2.1.
Mu13: nt 1–1146 of Kv2.1, nt 1138–1143 of Kv1.2, nt 1153-Stop of Kv2.1.
Mu14: nt 1–1182 of Kv2.1, nt 1174–1176 of Kv1.2, nt 1186–1191 of Kv2.1, nt 1183–1185 of Kv1.2, nt 1195-Stop of Kv2.1.
Mu15: nt 1–1209 of Kv2.1, nt 1201–1203 of Kv1.2, nt 1213-Stop of Kv2.1.
Mu16: nt 1–1224 of Kv2.1, nt 1216–1218 of Kv1.2, nt 1228–1230 of Kv2.1, nt 1222–1224 of Kv1.2, nt 1234–1239 of Kv2.1, nt 1231–1233 of Kv1.2, nt 1243-Stop of Kv2.1
Mu17: nt 1–1248 of Kv2.1, nt 1240–1245 of Kv1.2, nt 1255-Stop of Kv2.1

DNA sequences amplified by the polymerase chain reaction were verified by sequencing using the BigDye terminator cycle sequencing kit (Applied Biosystems, Foster City, CA). The sequence reactions were analyzed on an ABI 377 or Prism 310 automated sequencer (Applied Biosystems).

The cDNA encoding for the potassium channel subunits rat Kv1.2, human Kv2.1, and their chimeras were transcribed to cRNA using a commercial kit (mMessage mMachine; Ambion, Austin, TX) and T7 RNA polymerase. Denaturating agarose gel electrophoresis was used to check the quality of cRNA product of each reaction and to quantify the yield.

Preparation of Oocytes and Cell Lines. South African clawed frogs (*Xenopus laevis*) were anesthetized in ethyl *m*-aminobenzoate (Sandoz, Basel, Switzerland) and small sections of the ovary were removed surgically. Oocytes (stage V or VI; Dumont, 1972) were injected with 0.1 or 1.0 ng of cRNA in 50 nl of distilled water and were maintained under tissue culture conditions at 20°C until used for experiments. The tissue culture solution was a modified Barth medium (88 mM NaCl, 1 mM KCl, 1.5 mM $CaCl_2$, 2.4 mM $NaHCO_3$, 0.8 mM $MgSO_4$, 5 mM HEPES, pH 7.4) that was supplemented with penicillin (100 IU/ml) and streptomycin (100 μg/ml).

For the electrophysiological recordings on membrane patches, part of or all of the follicular tissues were removed from the oocytes. The outer part of the follicular tissues was stripped off some hours after injection of cRNA with forceps (defolliculation). The remaining follicular tissues were removed manually just before the electrophysiological investigation after shrinkage in a "stripping solution" (200 mM K-aspartate, 20 mM KCl, 1 mM $MgCl_2$, 10 mM EGTA, and 10 mM HEPES, pH 7.4 (Methfessel et al., 1986).

For heterologous expression in cell lines, we used CHO cells expressing human Kv2.1 and rat Kv1.2 channels (Zhu et al., 1999). The cDNA were subcloned into pcDNA3, and CHO cells were transfected using LipofectAMINE following the manufacturer's protocol (Invitrogen, Carlsbad, CA). In all experiments, pcDNA3-GFP was cotransfected together with pcDNA3-Kv2.1 to mark the CHO cells expressing Kv channel subunits with green fluorescent protein fluorescence. Briefly, 200 μl of Opti-MEM I containing a total of 0.1 μg DNA (Kv2.1) or 1.0 μg DNA (Kv1.2) together with 3 μl of LipofectAMINE and 0.5 μg of enhanced green fluorescent protein were used to transfect 4×10^5 cells in a 35-mm tissue culture plate. The lipid-DNA complex solution was replaced after 5 to 6 h of incubation by minimal essential medium-α.

Electrophysiological Techniques. For investigations of oocytes with the two-electrode voltage-clamp technique, microelectrodes were made from borosilicate glass and had resistances of 0.5 to 1 MΩ for the current electrodes and 1 to 2 MΩ for the potential electrodes when filled with 3 M KCl. The holding potential was −80 mV, and command potentials were applied up to a potential of +80 mV. Tail currents were obtained by stepping from +20 mV to potentials of −40 to −120 mV. The control bath fluid was a Ringer solution (115 mM NaCl, 2 mM KCl, 1.8 mM $CaCl_2$, and 10 mM HEPES; pH 7.2. Propafenone (PROP as chloride salt; Sigma, Deisenhofen, Germany) in concentrations of 1 to 2000 μM and tetraethylammonium (TEA as chloride salt; Merck-Schuchardt, Hohenbrunn, Germany) was added to the bath solution and applied at least 30 s before eliciting currents. Solutions were applied with a concentration-clamp technique (Madeja et al., 1991), allowing an exchange of more than 90% of the extracellular solution within <10 ms. All experiments were performed at days 3 and 4 after injection of cRNA and were carried out at room temperature (22 ± 1°C).

Investigations of oocytes with the patch-clamp technique were done on excised membrane patches in the outside-out or inside-out configurations. The patch pipettes had tip diameters between 1 and 4 μm and resistances between 2 and 5 MΩ. The holding potential was −80 mV, and command potentials were applied up to a potential of +20 mV. Solutions were applied with the double-barrel flow pipette method (Johnson and Ascher, 1987). In outside-out membrane patch investigations, the bath fluid was the above-mentioned Ringer solution, and the patch pipettes were filled with a solution of the composition 100 mM KCl, 10 mM EGTA, and 10 mM HEPES, pH 7.2. For investigations on inside-out membrane patches, the solutions were exchanged correspondingly.

Channels expressed in CHO cells were studied with the patch-clamp technique in the whole-cell configuration. The holding potential was −80 mV, and command potentials were applied to a potential of +60 mV. The patch pipettes (resistances between 1.8 and 3 MΩ) were filled with a solution of the composition 160 mM KCl, 0.5 mM $MgCl_2$, 10 mM HEPES, and 2 mM ATP-Na_2, pH 7.2. The bath solution was composed of 135 mM NaCl, 5 mM KCl, 2 mM $MgCl_2$, 2 mM $CaCl_2$, 10 mM sucrose, 5 mM HEPES, and 0.01 g/liter phenol red, pH 7.4. PROP was added to the bath solution, giving concentrations from 0.3 to 100 μM and was applied to the cells using a hydrostatic superfusion system (50 to 100 μm distance to the cell under investigation). Currents were recorded at room temperature at days 2 and 3 after transfection of the cells.

Data Acquisition and Analysis. The potassium currents obtained in two-electrode recordings were low-pass filtered at 1 kHz and were transferred to a computer system (pClamp; Axon Instruments, Union City, CA). The amplitudes of the total outward currents were corrected for leakage. Leakage currents and capacitive transients were subtracted online using a p/−4 pulse protocol.

The potassium current amplitude was measured at the peak of current obtained during the depolarizing voltage step. Conductance-voltage relations were obtained by normalizing the conductance data to the maximal value under control conditions and by fitting the data to the Boltzmann equation $y = G_{max}\,(1 + \exp\,[(V_{1/2} - V)/b])$, where y is the normalized conductance, G_{max} is the normalized maximal conductance, $V_{1/2}$ is the potential of the half-maximal conductance, V is the voltage, and b is the slope factor. The decay of tail currents was fitted with monoexponential functions. Concentration-response curves were determined by fitting the mean current values at different PROP concentrations to the Langmuir equation $y = (K_D/c)^{n_H}/[1 + (K_D/c)^{n_H}]$, where y is the fraction of control current, K_D is the half-blocking concentration, c is the concentration of PROP, and ^{n_H} is the Hill coefficient.

The voltage dependence of block was determined using the K_D values that were obtained for these calculations from the fractional current (f), measured as the current in the presence of propafenone (I_{PROP}) at a concentration [D] of 100 μM or 2 mM and under control conditions (I_{CTRL}) at the end of the voltage step: $f = I_{PROP}/I_{CTRL}$ and $K_D = [D] \times f/(1 - f)$. The fractional electrical distance (δ) (i.e., the fraction of the transmembranous electrical field sensed by a single positive charge at the binding site) was determined by fitting the K_D values with the equation $K_D = K_{D(0mV)} \times \exp(-z\delta FV/RT)$. $K_{D(0mV)}$ represents the half-blocking concentration at the reference potential of 0 mV, V is the membrane potential, z is the charge of the molecule, F is the Faraday constant, R is the real gas constant, and T is the absolute temperature.

The potassium currents of CHO cells were low-pass filtered at 3 kHz, digitized using an analog-to-digital converter (HEKA Electronic, Lambrecht, Germany) and were stored with a sampling rate of 10 kHz. PROP-induced inhibition of the currents was quantified as inhibition of the steady-state current. K_D values were determined with the above-mentioned Langmuir equation.

The measured values are given as mean or mean ± S.E.M. Statistical significance was tested using a t test or a Mann-Whitney rank sum test. Values of $p < 0.01$ were taken as statistically significant. Curve fitting and all statistical procedures were performed using the program SigmaPlot (SPSS Science, Chicago, IL).

Results

Conductance Parameters. In agreement with previous results, outward currents mediated by Kv2.1 channels expressed in *X. laevis* oocytes appeared at potentials positive to −30 mV. The currents increased relatively slowly and did not significantly inactivate during the 500 ms test pulses (Fig. 1A, CTRL). PROP at a concentration of 100 μM decreased the outward currents over the entire potential range. At the most positive test pulses (+50 and +60 mV), a change in the activation kinetics became apparent (Fig. 1A, PROP; see the small hump at the beginning of the current traces). A fitting of the mean conductance values revealed a decrease of the

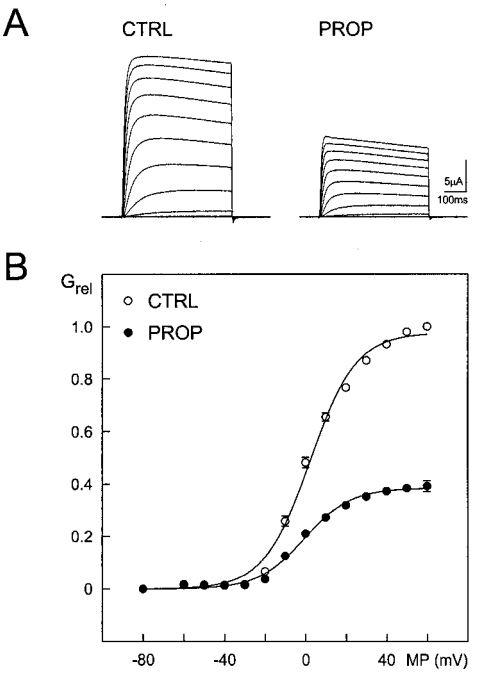

Fig. 1. Effect of PROP on Kv2.1 potassium currents. *X. laevis* oocytes. Potential steps from −80 to +60 mV under control conditions (CTRL, ○) and with PROP (100 μM, ●). A, original recordings. B, open probability curves of mean conductance values from 10 experiments. The conductance values (G_{rel}) were normalized to the respective maximal value under control conditions. The error bars indicate SEM. MP, membrane potential.

maximal conductance (G_{max}) by more than 60% (Fig. 1B). The conductance-voltage relation was not significantly affected with a shift of the potential of half-maximal conductance ($V_{1/2}$) of less than −3 mV (mean values: CTRL, 2.4mV; slope factor, 11.4 mV; PROP, −0.5 mV; slope factor, 11.4 mV).

Activation and Deactivation Kinetics. As can be seen from a comparison of the normalized current traces at +40 mV in Fig. 2A, the Kv2.1 current increased more rapidly with PROP compared with control conditions (Fig. 2A, left). The rise of current could be well fitted with monoexponential functions (except for the first few milliseconds of the test pulse; see Fig. 2A, left) at test potentials of +10 to +60 mV. A plot of the time constants as a function of the test voltage (Fig. 2A, right) showed that the time constants decreased from 44 ± 3 ms at +10 mV to 11 ± 1 ms at +60 mV (n = 5). In the presence of PROP, the time constants were decreased at all test potentials. The decrease was voltage-dependent and ranged from 30% at +10 mV to 42% at +60 mV. In line with this voltage dependence, a linear fit of the logarithm of the time constants in the range from +30 to +60 mV revealed 162 and 108 mV for a 10-fold change in time constants under control conditions and PROP, respectively (n = 5; data not shown). PROP did not alter the deactivation kinetics of Kv2.1 channels (Fig. 2B, left), which could be well described with monoexponential functions. Stepping from +20 mV to test voltages of −40 to −120 mV, the voltage dependence of deactivation time constants decreased from 17 ± 1 ms at −40 mV to 4 ± 1 ms at −120 mV (n = 5). In the presence of PROP, the time constants were not significantly different from the control values (Fig. 2B, right).

Kinetic and Voltage Dependence of Block. We analyzed the development of Kv2.1 current block in the presence of 100 μM PROP in comparison with control currents. Plotting this relative current against test pulse duration showed that the Kv2.1 current block developed rapidly within the first milliseconds of the test pulse and then increased more slowly during the rest of the pulse (Fig. 3A). Correspondingly, the decay could not be fitted with a monoexponential function but was described with the sum of two monoexponential functions with time constants of 14 and 901 ms at +60 mV (fit of normalized mean currents of five experiments). Extrapolating this fit of the development of block to zero time at the beginning of the test pulse indicated an initial block of <19% (Fig. 3A, hatched line). This observation supports the view that PROP mainly blocks the open Kv2.1 channel and that the efficacy of block increases with open probability. The block was apparently not use-dependent because the same block of current was obtained after 1, 10, or 30 voltage pulses during a 30-s application of PROP (data not shown, n = 5).

Next, we studied the contribution of the two different components of the block. At +60 mV, the fast component of block (Fig. 3A, dotted line) represented more than 89% of the block computed as the difference of the block after 0 and 500 ms. At

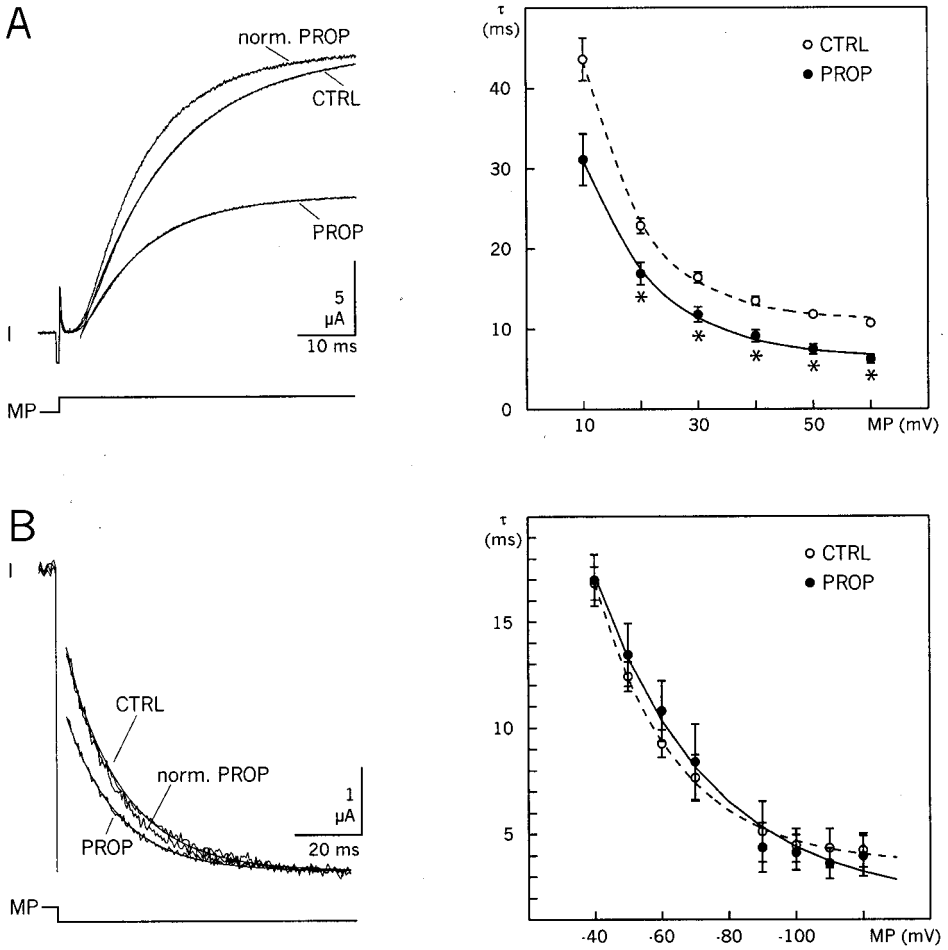

Fig. 2. Effect of propafenone (PROP) on current kinetics of Kv2.1 potassium channels. *X. laevis* oocytes. Currents (I) under control conditions (CTRL, ○) and with propafenone (100 μM, ●). MP, membrane potential. A, time course of current increase. Left, original recordings of potassium currents at +40 mV. The solid lines indicate the fit of currents with monoexponential functions. norm. PROP, currents with PROP normalized to the maximal current under control. Right, graphical evaluation of the time constants (τ) of current increase at different potentials. The data are given as mean ± S.E.M. of five experiments and are fitted with monoexponential functions. Asterisks mark statistically significant differences. B, time course of tail currents. Left, tail currents at a potential of −40 mV after 50-ms voltage steps to +20 mV. Except for the first 3 ms after the end of the voltage step, the tail currents were fitted with monoexponential functions. Right, graphical evaluation of the time constants (τ) of tail currents at different potentials; five experiments. Further explanation as in A.

+20 mV, the fast component slightly decreased to 82% of the block, thus suggesting a voltage dependence of the two components of block (data not shown). We therefore measured the two time constants of the block in the potential range from +20 to +80 mV (Fig. 3B). The fast time constant decreased steadily from 25 ± 7 ms at +20 mV to 14 ± 1 ms at +80 mV, whereas the slow time constants ranged between 1035 ± 256 ms and 1309 ± 282 ms. A linear regression was obtained for the correlation between the logarithm of the fast time constant and the voltage (p = 0.006; regression coefficient r = 0.90; Fig. 3B), whereas the slow time constants showed no voltage dependence (n = 5). Thus, the voltage- and time-dependent increase in block described by the fast time constants is consistent with a block of the channel in the open state. The additional slowly increasing block is probably independent of the channel state and might be caused, for example, by a diffusion-dependent increase of PROP concentration at the binding site (see *Discussion*).

In the open channel, the whole electric field has to decline from the internal to the external mouth of the channel pore, and because this field might affect the action of a blocking agent, we performed investigations on the voltage dependence of PROP block. The voltage dependence of block was calculated by the fraction of control current with propafenone in the potential range from −20 to +80 mV (Fig. 3C). The PROP-induced block increased with positive-going potentials as indicated by a steady decrease of the half-blocking concentrations (K_D) with positive-going potentials. The fractional electrical distance (i.e., the fraction of the transmembranous electrical field sensed by the drug at the binding site, referenced to the intracellular side of the channel) was calculated at potentials from +50 to +80 mV. In this potential range, the open probability was roughly maximal (change of maximal conductance <7%; n = 5; Fig. 3C, hatched line) and the endogenous currents of the oocytes were small (<0.8 μA up to +80 mV in water-injected oocytes; n = 3; data not shown). A fit of the half-blocking concentrations (K_D) at these potentials with the measured K_D of 111 ± 13 μM PROP at the reference potential of 0 mV ($K_{D\ 0mV}$) yielded an electrical distance $z\delta_1$ = 0.13 ± 0.02 (n = 5; Fig. 3C). At the potential of 0 mV, however, the open probability was low (45% of the maximal value), suggesting that the theoretical K_D for maximal open probability could yield a smaller value than the computed one. The values were therefore refitted with the assumption of an unknown K_D at 0 mV. The fit revealed an electrical distance $z\delta_2$ = 0.11 ± 0.02 and a $K_{D\ 0mV}$ = 107 ± 17 μM PROP (Fig. 3C). As expected, the fitted $K_{D\ 0mV}$ value was lower than the measured one, but the difference was small, indicating that at this (and at more positive) potential, the increase in open probability did not contribute strongly to the increase in block.

Because the block by PROP could only be well described with the sum of two exponential functions and because only the fast component might be caused by changes in the channel's state, we also calculated the fractional electrical distance using the limit values of the fast monoexponential fit of block. With these values, we obtained an electrical distance $z\delta_3$ = 0.14 ± 0.07 (data not shown; n = 5).

Effects on Isolated Membrane Patches and Transfected Mammalian Cells. To test the hypothesis that PROP blocks open Kv2.1 channels from the inside, we applied 10 μM PROP to membrane patches excised from oocytes expressing Kv2.1 channels. As a first step, we measured current-voltage relations from −80 to +20 mV in inside-out membrane patches (Fig. 4A). As observed for the whole oocyte, the threshold for Kv2.1 current activation was between −40 and −30 mV. Under these conditions, PROP at a concentration of 10 μM blocked much more than half of the current (Fig. 4A). Thus, the blocking effect seemed to be much larger than in whole oocytes (compare Figs. 1 and 3C),

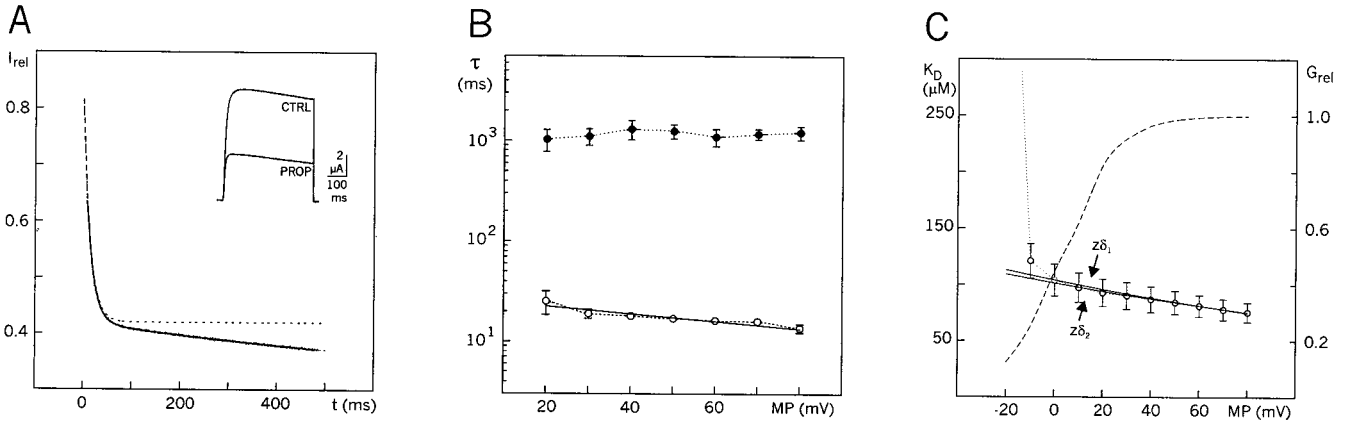

Fig. 3. Time course and voltage dependence of the block of Kv2.1 potassium currents by PROP. *X. laevis* oocytes. A, change of fractional current (I_{rel}) [i.e., fraction of current with PROP (100 μM) relative to current under control conditions (CTRL)] with the duration (t) of voltage steps to +60 mV (except for the first 8 ms). The trace is the mean of six experiments. Hatched line, fit of I_{rel} with biexponential functions. The fit is shown from 0 to 500 ms of the voltage step. Dotted line, fraction of I_{rel} obtained from the faster time constant of the biexponential fit. Inset, original recording of currents at +60 mV. B, voltage dependence of time constants (τ) of biexponential fits used to describe the time course of block as shown in A. Fast (○) and slow time constants (●) are shown as mean ± S.E.M. of five experiments in the potential range from +20 to +80 mV. The solid line indicates the linear regression for the correlation between the logarithm of the time constant and the voltage (P = 0.006; regression coefficient r = 0.90). MP, membrane potential; C, voltage dependence of fraction of block. The half-blocking concentrations (K_D) at different potentials are given as mean ± S.E.M. of five experiments (○, dotted line). The hatched line gives the open probability curve obtained by fitting the relative conductance values (G_{rel}) current amplitude with a Boltzmann equation. The fractional electrical distance ($z\delta$) (i.e., the fraction of the transmembranous electrical field sensed by a substance with the positive charge z at the binding site) was determined as described under *Data Acquisition and Analysis*. The fit was performed with the measured $K_{D(0mV)}$ value of 111 ± 13 μM ($z\delta_1$ = 0.13 ± 0.02) and with an unknown $K_{D(0mV)}$ ($z\delta_2$ = 0.11 ± 0.02, $K_{D(0mV)}$ = 107 ± 17 μM; n = 5, solid lines).

suggesting that the reduced sensitivity in whole oocytes is most probably caused by reduced access to the channel's binding site (Madeja et al., 1997; Rolf et al., 2000). The persistence of the PROP effect in isolated membrane patches suggests, however, that intracellular messengers or factors of the cell are not critically involved in the action of PROP and that the block of Kv2.1 currents is induced by PROP directly.

To study the sensitivity to PROP in a mammalian expression system, we measured the K_D values in CHO cells expressing Kv2.1 channels (and for comparison also Kv1.2 channels). Voltage steps were elicited from −80 to +60 mV (Fig. 4B). The K_D values were 1.2 ± 0.3 μM for Kv2.1 (n = 16) and 9.8 ± 4.9 μM for Kv1.2 (n = 21; Fig. 4B). In oocytes, however, the K_D values were 91 ± 12 μM for the Kv2.1 channel (n = 8) and 953 ± 88 μM for the Kv1.2 channel (n = 7; data not shown). Thus, the two Kv channels expressed in the mammalian cells showed a much higher sensitivity to PROP compared with their sensitivity in oocytes, but the relative differences in sensitivity between Kv2.1 and Kv1.2 channels were similar in both expression systems ($K_{DKv2.1}$/$K_{DKv1.2}$: 0.12 in CHO cells and 0.10 in oocytes).

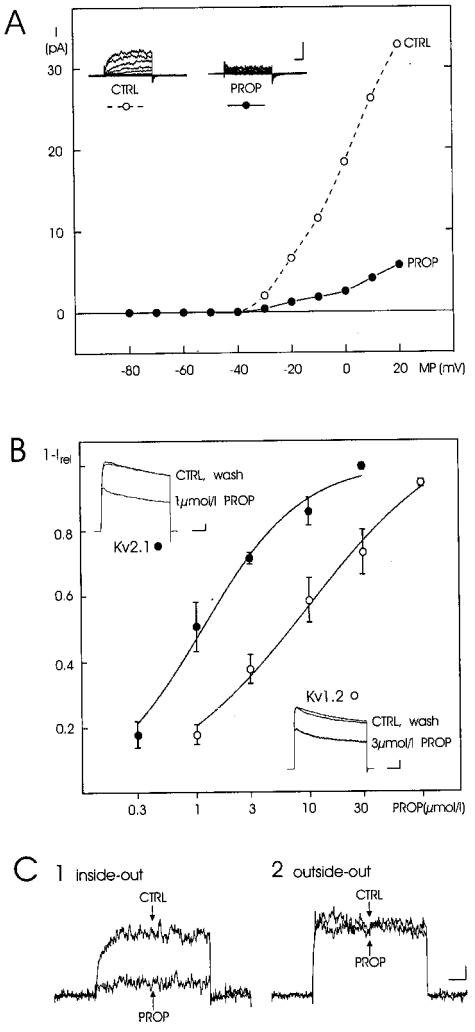

Fig. 4. Effect of PROP on excised membrane patches and mammalian cells with Kv2.1 and Kv1.2 potassium channels. CTRL, control conditions. A, current-voltage relations of Kv2.1 channels in inside-out patches of oocytes of *X. laevis*. PROP was applied at a concentration of 10 μM. Inset, original recordings used for the graphical evaluation. Calibrations, 20 pA and 90 ms. CTRL, control conditions; I, potassium current. B, concentration-response curves for PROP of Kv2.1 (●) and Kv1.2 currents (○) in heterologously transfected CHO cells. The symbols represent fraction of inhibition of potassium current as mean ± S.E.M. of 16 (Kv2.1) and 21 experiments (Kv1.2). Data were fitted to a Langmuir equation. I_{rel}, fraction of current with PROP relative to current under control conditions; 1 − I_{rel}, fraction of inhibition. The insets show original recordings. Calibrations; 1 nA and 100 ms. C, effect of PROP on Kv2.1 potassium currents in membrane patches of oocytes of *X. laevis* in the inside-out (1) and outside-out (2) configurations. Superposed original recordings before (CTRL) and with PROP (1 s after begin of application). Calibrations, 6 pA and 90 ms.

To test PROP action on the intracellular or extracellular side of the membrane, we applied PROP to membrane patches of oocytes in both the inside-out and outside-out configuration (Fig. 4C). The excised patches contained only a few channels in our experiments; thus, it was not possible to make conclusions about channel kinetics. We elicited Kv2.1 currents by a voltage step to +20mV. To avoid contaminating effects caused by PROP traversing the cell membrane, we elicited the voltage steps 1 s after begin of PROP application to the membrane patches. With this protocol, 10 μM PROP applied to inside-out patches markedly reduced Kv2.1 current amplitudes (Fig. 4C, 1; n = 4). By contrast, PROP application to outside-out patches did not significantly affect Kv2.1 current amplitudes (Fig. 4C, 2; n = 5).

Mutagenesis Experiments. As reported previously (Rolf et al., 2000), Kv1.2 channels in oocytes of *Xenopus laevis* are relatively resistant to block by PROP. Kv1.2 mean current amplitudes at +40 mV (i.e., 50 mV positive to the threshold potential) were reduced by only 9%, whereas Kv2.1 currents were decreased by 59% (Fig. 5A; n = 6 to 9). We took advantage of this observation and constructed a systematic set of Kv2.1/Kv1.2 chimeras to screen the Kv2.1 channel domains for high-affinity PROP binding sites in the oocyte expression system. We tested for insensitivity of the Kv2.1 channel to also discover a possible composite site of action. In a first step, the Kv2.1 amino terminus (Mu1), the first (Mu2) and second half (Mu3) of the membrane-inserted Kv2.1 core domain and the Kv2.1 carboxy terminus (Mu4) were replaced by Kv1.2 (Fig. 5B; n = 5 to 9). Current amplitudes at +40 mV of chimeras Mu1, Mu2, and Mu4 were reduced by PROP in a similar manner to those of wild-type Kv2.1 channels, whereas the current amplitudes of chimera Mu3 were as insensitive to PROP as wild-type Kv1.2 channels. These results suggest a high-affinity binding site for PROP to domain(s) in the second half of the Kv2.1 membrane-spanning core region extending from segment S4 to S6.

Next, we analyzed the S4 to S6 region in more detail (Fig. 5C; n = 5 to 9). Replacement of segment S4 (Mu5), segment S5 (Mu7), or the intracellular S4-S5 linker (Mu6) did not transfer PROP insensitivity to the Kv2.1 channel. Transfer of the S5-S6 linker region (Mu8), as well as replacement of segment S6 (Mu9), reduced the sensitivity of Kv2.1 channels to PROP to the level of wild-type Kv1.2 channels. Thus, the site of action can be assumed to be located at those parts of the channel molecule that have been shown to form the pore proper of a potassium channel (Doyle et al., 1998). It should be noted, however, that in addition to the mutations mentioned above (Mu3, Mu8, and Mu9), smaller but statistically significant reductions of the PROP-induced decrease of current were found for the mutants Mu1, Mu4, and Mu6 (Fig. 5, daggers), thus suggesting some effect of the intracellular termini and the intracellular linker S4-S5.

The results suggest that the amino acid residues forming

the S5-S6 linker region and segment contain the PROP binding site of the Kv2.1 channel. At first, we exchanged amino acid residues in the Kv2.1 S5-S6 linker region and measured the change in maximal conductance of the mutants. Concerning the linker region between segments S5 and S6 (Fig. 6A, $n = 6$ to 10), the exchange of the chains of extracellular amino acids flanking the intramembraneous pore region (Doyle et al., 1998; Fig. 6A, p) did not reduce the PROP sensitivity significantly (Mu10). Within the P-region, however, the exchange of a group of three amino acids (threonine 371, isoleucine 372, and threonine 373; Mu12) and another group of two amino acids (isoleucine 383 and tyrosine 384; Mu13) for those of the Kv1.2 channel strongly reduced the channel's sensitivity to PROP (differences from Kv1.2 statistically not significant; Fig. 6A, asterisks), whereas the other exchange in the P-region (alanine 366 and serine 367; Mu11) had no statistically significant effect (Fig. 6A).

To study the concentration dependence of the PROP action on these mutants, we measured the K_D values at potentials of +60 mV by applying PROP in concentrations from 1 to 1000 μM. Both mutants showed an insensitivity to PROP (Mu12, K_D, 2909 ± 614 μM, $n = 7$; Mu13, K_D, 2180 ± 512 μM, $n = 6$) which was the same or even greater than of the of the Kv1.2 channel (K_D = 953 μM) and clearly distinct of the Kv2.1 channel (K_D = 91 μM).

Because the residues 371 to 373 and 383 to 384 are located in regions of the molecule that have been associated with the binding site of TEA in other potassium channels (Yellen et al., 1991; see *Discussion*), we tested the effect of TEA on the mutants. Similar to PROP, the Kv2.1 channel was more sensitive to TEA than the Kv1.2 (reduction of G_{max} by 20 mM TEA: Kv2.1, 67 ± 3%, $n = 6$; Kv1.2, 20 ± 3%, $n = 5$; data not shown). Both mutants of the P-region had a reduced PROP sensitivity (Mu12 and Mu13) and also a decreased sensitivity to TEA (reduction of G_{max}: Mu12, 37 ± 2%; Mu13, 2 ± 1%, $n = 6$ each; differences to Kv2.1 statistically significant; data not shown).

In a last set of mutants, we successively replaced Kv2.1 amino acid residues in S6 with those of Kv1.2 (Fig. 6B, Mu14 to Mu17). None of the current amplitudes of these mutants was reduced by PROP application as strongly as those of Mu9 or of wild-type Kv1.2 channels (Fig. 6B). Mu14 current amplitudes were as sensitive to PROP as wild-type Kv2.1 channels. In contrast, the current amplitudes associated with Mu15, Mu16, and Mu17 were significantly reduced by PROP but did not reach the PROP sensitivity of wild-type Kv1.2 channels.

Finally, we measured the fractional electrical distance $z\delta_1$ (in the potential range from 0 to +60 mV) for Kv1.2 and Mu10 to Mu17. Effects of PROP on voltage dependence of open probability were estimated by the shifts of $V_{1/2}$ in the presence of 100 μM PROP. For all channels, PROP induced shifts to negative potentials. The shift ranged between −0.3 ± 0.2 mV (Mu12) and −2.7 ± 0.3 mV (Mu17); the only exception was Mu14 with a shift of −6.2 ± 0.7 mV. The calculations of the fractional electrical distance yielded almost unchanged values for Mu14 ($z\delta_1 = 0.14 \pm 0.01$, $n = 8$) and Mu17 ($z\delta_1 = 0.13 \pm 0.02$, $n = 6$) compared with the Kv2.1 wild-type ($z\delta_1 = 0.13$, see above), but reductions for Mu10 ($z\delta_1 = 0.06 \pm 0.01$, $n = 7$), Mu11 ($z\delta_1 = 0.05 \pm 0.01$, $n = 8$), Mu15 ($z\delta_1 = 0.06 \pm 0.02$, $n = 8$), and Mu16 ($z\delta_1 = 0.10 \pm 0.04$, $n = 7$). Because Mu12 and Mu13 showed only small effects with 100 μM PROP, measurements were made with the concentration of 2000 μM PROP. The fractional electrical distances so obtained were larger than those of Kv2.1 and yielded $z\delta_1 = 0.15 \pm 0.03$ for Mu12 ($n = 6$) and $z\delta_1 = 0.21 \pm 0.03$ for Mu13 ($n = 7$). For the interpretation of these values, however, it must be noted that, especially for Mu13, the high PROP concentration caused a significant negative shift (Mu13, −7.5 ± 1.2 mV, $n = 7$; Mu12, −3.1 ± 1.0, $n = 6$), which, in principle, could lead to increased values of $z\delta_1$.

In summary, amino acid residues in the P-region and in the S6 segment reduced the PROP sensitivity of the Kv2.1 channel. A complete transfer of PROP insensitivity was obtained by exchanging the amino acids 371 to 373 and 383 to 384 of the P-region of the Kv2.1 channel. Furthermore, several amino acids of the S6 segment (404, group 409/411/414 and group 417/418) were found to reduce the sensitivity of the Kv2.1 channel to PROP.

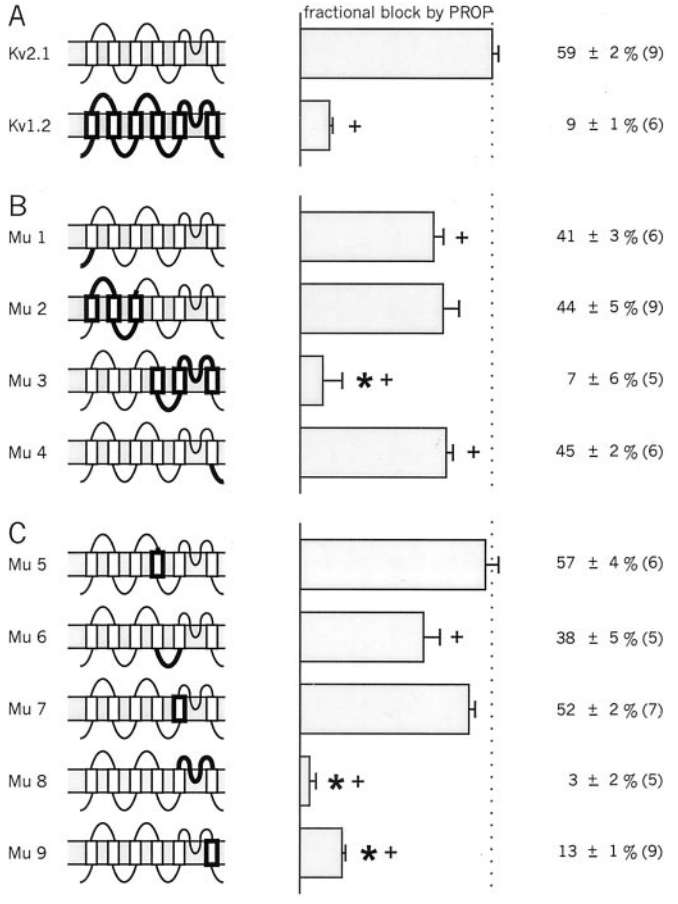

Fig. 5. Effect of PROP (100 μM) on potassium currents of chimeric channels obtained from Kv1.2 and Kv2.1 wild-type channels. *X. laevis* oocytes. The schematic drawings represent the structure of the wild-type and mutant channels (Mu1 to Mu9). The bars and numbers show the current percentage reduction 50 mV positive to the threshold potential (mean ± S.E.M.). The numbers in brackets indicate the number of experiments. Asterisks, no statistically significant difference from the Kv1.2 channel; Daggers, statistically significant difference from the Kv2.1 channel. Wild-type channels (A), chimeras with exchanges of larger parts of the channel (B), and chimeras with exchanges of single segments or linkers in the region S4 to S6 (C).

Discussion

The present study suggests 1) that PROP decreases the Kv2.1 potassium current by an open-channel block, 2) that PROP acts from the intracellular side of the membrane, and 3) that several residues of the pore region and of segment S6 determine the sensitivity to PROP.

Open-Channel Block. Three findings of the present study suggest a blockade in the open state of the channel: 1) the increase of block with time of activation, 2) the kinetics of current increase, and 3) the voltage dependence of block. Thus, almost no block of current was found at the beginning of the voltage pulse, and the block increased with time. The current increase with PROP was faster than under control conditions, suggesting a blocking effect of PROP that increases with time (Mergenthaler et al., 2001), although a direct effect of PROP on channel kinetics cannot be ruled out. Finally, the increase in block with positive-going potentials suggests a correlation between block and open probability of the channel. Taken together, these findings allow the conclusion that PROP blocks the Kv2.1 channel in the open state. This is consistent with blocking mechanisms of PROP found for Kv1.5 (Franqueza et al., 1998) and HERG channels (Mergenthaler et al., 2001).

Intracellular Side of Action. The conclusion that PROP acts from the intracellular side of the membrane is based on two findings: 1) the calculation of the electrical distance and 2) the efficacy of PROP in excised inside-out patches.

The calculation of the fractional electrical distance (δ) (i.e., the fraction of the transmembranous electrical field sensed by a single positive charge at the binding site) yielded a value δ of 0.11 to 0.14 for PROP. However, PROP can be assumed to be only partly charged in the cytoplasm of the oocyte; this fact needs to be considered in estimating the electrical distance. With a pK value of 8.8 for PROP (Mergenthaler et al., 2001) and an intracellular pH value of 8.2 in the oocyte (Kauder et al., 1991), only 80% of the intracellular propafenone is positively charged. Assuming that PROP blocks the potassium channel in both the charged and uncharged forms with the same efficacy, a mean charge $z = 0.8$ could increase the electrical distance to $\delta_1 = 0.16$, $\delta_2 = 0.14$, and $\delta_3 = 0.18$. These values are similar to those found for TEA (internal application; $\delta = 0.16$; Choi et al., 1993), quinidine ($\delta = 0.19$; Snyders et al., 1992), and bupivacaine ($\delta = 0.16$; Valenzuela et al., 1995), whose site of action has been attributed to the internal mouth of the potassium channel based on the results of mutagenesis experiments (Yellen et al., 1991; Yeola et al., 1996; Franqueza et al., 1997).

In experiments with excised patches, we obtained a blocking effect after rapid application to the intracellular side of the cell membrane but not to the extracellular side. Because this experimental approach minimized possible contributing effects of diffusion and/or transport across the cell membrane, the findings suggest an action of PROP at intracellular regions of the channel molecule.

It was not the aim of the present study to determine by which mechanism PROP can enter the cell. The finding that the amount of block at the Kv2.1 channel is independent of the time the channel is activated, however, suggests that drug transport across the cell membrane is not associated with channel activity; thus, structures of the channel molecule are most probably not involved in this transport. A simple diffusion process through the cell membrane, however, might be possible and is in line with the quite slow increase in block with time (less than 15% of block after 1 s of PROP application and 60% after 10 s; data not shown). Thus, uncharged PROP molecules (pK value 8.8) might enter the cell membrane compartment and might move transversely into the intracellular space as charged molecules because of pH-dependent equilibria and driven by the concentration gradients. Such a mechanism is supported by the finding that an increase of extracellular pH improved the presumably intracellular blocking efficacy of PROP at the HERG channel (Mergenthaler et al., 2001).

Molecular Sites of Action of the Channel Molecule. Several regions have been found that when replaced by the corresponding parts of the Kv1.2 channel, reduced the sen-

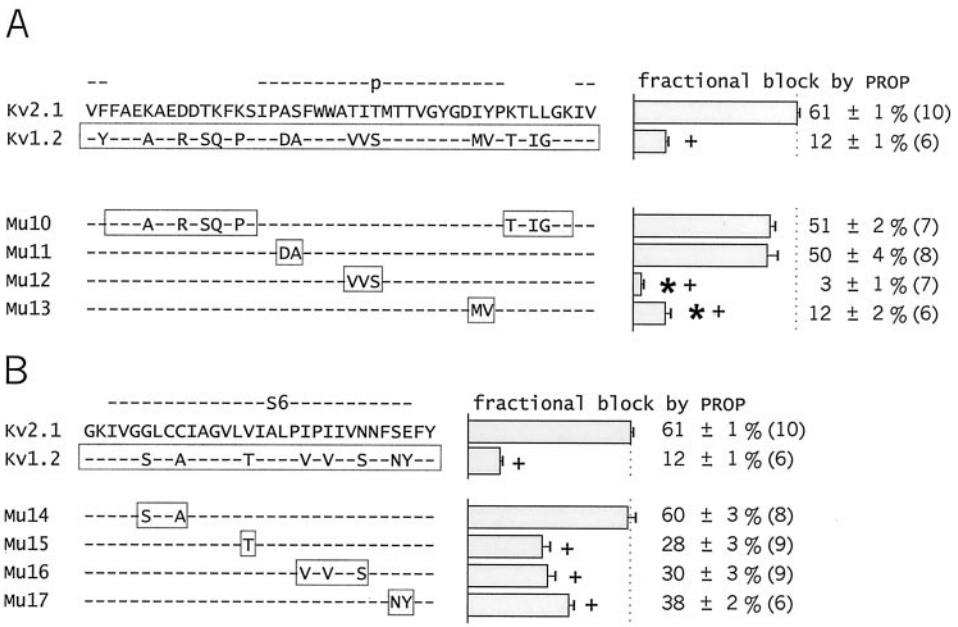

Fig. 6. Effect of PROP (100 μM) on potassium conductance of mutated Kv2.1 channels representing substitutions by the corresponding residues of the Kv1.2 channel in the linker S5-S6 (A) and in the S6 segment (B). *X. laevis* oocytes. The left part shows the amino acid sequences of the wild-type and mutated channels (Mu10 to Mu17). For the Kv1.2 channel and the mutated channels, only the residues differing from Kv2.1 are given. The bars and numbers show the percentage reduction of maximal conductance (mean ± S.E.M.). The numbers in brackets indicate the number of experiments. Asterisks, no statistically significant difference from the Kv1.2 channel; Daggers, statistically significant difference from the Kv2.1 channel.

sitivity of the Kv2.1 channel. Replacement of the intracellular termini and the intracellular linker S4-S5 induced moderate effects. Because there is growing evidence that these parts of the channel form an intracellular compartment placed near the membrane-associated part of the channel pore (hanging gondola model; Kobertz et al., 2000), the intracellular termini and the S4-S5 linker might impair the access of PROP to its proper site of action in the internal mouth of the channel.

A complete abolition of the PROP sensitivity of Kv2.1 (to the level of Kv1.2) was found with exchanges of the linker S5-S6, as well as with the S6 segment itself. Based on X-ray analysis of the KcsA potassium channel, these parts can be assumed to form the inner wall of the pore proper (Doyle et al., 1998).

Within the linker between segments S5 and S6, the replacement of amino acids 372 to 374 by the corresponding residues of Kv1.2 abolished the PROP sensitivity to the level of the Kv1.2 channel. If the amino acid sequence of the Kv2.1 channel is transferred onto the structure of the KcsA channel (Doyle et al., 1998), these residues form the intracellularly orientated part of the pore helix (Fig. 7, black points). Although these residues have no direct access to the internal vestibule of the analyzed KcsA channel, which is most probably in a closed state, they are near the vestibule and might be accessible after transition to the open state. On the other hand, it cannot be excluded that the three-dimensional structure of the Kv2.1 channel differs slightly from that of KcsA channel, thus exposing these residues into the inner vestibule, or that these residues only affect or shield the binding site.

Studies of other substances on the HERG channel showed a reduction of the sensitivity to dofetilide and verapamil when the serine residue 620 corresponding to residue 373 of the Kv2.1 was mutated (Ficker et al., 1998; Zhang et al., 1999; Fig. 7). A neighboring residue corresponding to amino acid 376 in Kv2.1 (Fig. 7, gray point) and forming the lowest end of the pore helix in the KcsA channel (Doyle et al., 1998), however, has been found to affect the sensitivity to several drugs, including bupivacaine and quinidine (Franqueza et al., 1997; Yeola et al., 1996) in the Kv1.5 channel and the antiarrhythmic drug MK-499 in the HERG channel (Mitcheson et al., 2000). The region corresponding to residues 372 to 374 in Kv2.1, which, in parallel to PROP action might also affect the sensitivity to these drugs, has unfortunately not been probed.

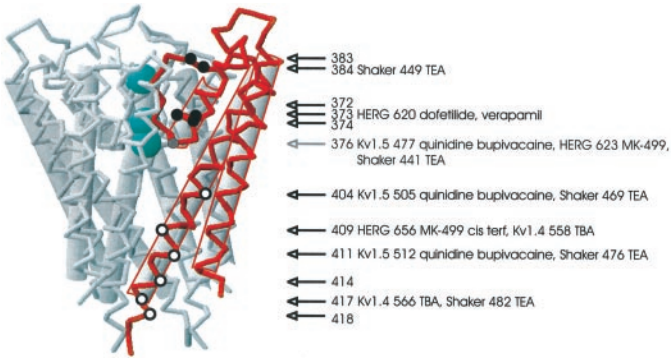

Fig. 7. Model of the pore region of the Kv2.1 channel derived from the structure of the KcsA channel after Doyle et al. (1998). The presentation of the structure is based on the Cn3D program (National Center for Biotechnology Information, Bethesda, MD). The α backbone is shown lined with the schematic helices. One of the four subunits is shown in red. The residues corresponding to the amino acids in Kv2.1 abolishing and reducing the sensitivity to propafenone are marked as ● and ○, respectively. The numbers of these amino acids are given on the right together with corresponding residues in other channels affecting drug sensitivity to bupivacaine, cisapride (cis), dofetilide, MK-499, quinidine, terfenadine (terf), tetrabutylammonium (TBA), TEA, verapamil (Yellen et al., 1991; Choi et al., 1993; Yeola et al., 1996; Franqueza et al., 1997, 1998; Ficker et al., 1998; Zhang et al., 1999; Mitcheson et al., 2000; Zhou et al., 2001). The gray dot and arrow mark residue 376, shown to be important for drug sensitivities in other channels (Yellen et al., 1991; Choi et al., 1993; Yeola et al., 1996; Franqueza et al., 1997; Mitcheson et al., 2000).

Results of TEA support the hypothesis of slightly varying sites of action for drugs in different channels. In the Shaker channel, amino acids corresponding to residues 372 to 374 of Kv2.1 have not been found to be associated with the sensitivity to TEA (Choi et al., 1993), whereas strong effects appeared for the amino acids 440 and 441, corresponding to the residues 375 and 376 of Kv2.1 (Yellen et al., 1991; Choi et al., 1993). The opposite is found for the Kv2.1 channel. The residues 375 and 376 cannot be responsible for differences in TEA sensitivity because the corresponding residues are identical in Kv1.2 and Kv2.1 channels (Fig. 6), whereas in our study, mutations of the residues 372 to 374 strongly affected the TEA sensitivity. These data, however, do not prove varying binding sites for TEA and PROP in the Shaker and Kv2.1 channel because it cannot be excluded that the residues 375 and 376 form the binding site, with nearby residues 372 to 374 allowing or preventing access of the drugs.

The second group of amino acids in the S5-S6 linker able to abolish the sensitivity of Kv2.1 to PROP concerns the residues 383 and 384 (Fig. 7, black points). The residue corresponding to the amino acid 384 in Kv2.1 has been found to affect the sensitivity to externally applied TEA in Shaker (residue 449; Yellen et al., 1991). Correspondingly, the mutation of these residues in Kv2.1 strongly reduced the effect of TEA in the present study. Thus, it is likely that this region is important for the blocking effects of both TEA and PROP. Based on the structure of the KcsA channel, however, these residues can be assumed to be located on the extracellular side of the channel molecule near the outer channel mouth. This is not in agreement with our findings in excised patches, because in these experiments, an application of PROP to the extracellular side did not yield a blocking effect. Although the reason for this discrepancy is not clear, that the site of mutation might not necessarily be the site of drug binding has to be considered. Indirect effects such as changes in channel conformation (allosteric mechanisms) or opening kinetics might be induced, which could have strong effects on drug action. Furthermore, although unlikely, it cannot be excluded totally that these amino acids become accessible from the intracellular side with the opening of the pore. In summary, however, the data do not allow postulation of an external binding site for PROP (or TEA) at the Kv2.1 channel.

We have found several amino acids of the intracellularly orientated part of the segment S6 of the Kv2.1 channel that decrease the PROP sensitivity strongly (residue 404, group 409/411/414 and group 417/418; Fig. 7, ●). Some of these amino acids affected the sensitivity to quinidine, bupivacaine, TEA, MK-499, cisapride, terfenadine, and tetrabutylammonium in other channels (Choi et al., 1993; Yeola et al., 1996; Franqueza et al., 1997; Mitcheson et al., 2000; Zhou et al., 2001). In these studies from the literature, however, other mutations of S6 have also been described to affect drug

sensitivity (e.g., mutations of residues corresponding to residues 401, 402, 405, 407, 408, and 413). It cannot be concluded based on our data whether the changes in S6 affect the binding site of PROP or the access of PROP to the site of action. The changes of the fractional electrical distance for some of these mutants, however, suggest that the binding pocket for PROP might be impaired with residues facing the inner vestibule of the channel.

Taking all the findings into consideration, we suggest that PROP enters the cell by diffusion across the cell membrane and acts from the intracellular side. PROP blocks the Kv2.1 channel in the inner vestibule of the channel while it is in the open state. The access of PROP to its binding site can be impaired by intracellular parts of the channel (linker S4-S5, intracellular C and N terminus). Residues of segment S6 might contribute to this impairment or to the formation of the binding site, which most probably includes the lower part of the pore helix.

Acknowledgments

We are thankful to Prof. Olaf Pongs for supporting us with cRNA of the wild-type and chimeric channels, for fruitful discussions, and for reviewing the manuscript. We are grateful to B. J. Corrette for English corrections.

References

Barry DM, Trimmer JS, Merlie JP, and Nerbonne JM (1995) Differential expression of voltage-gated K^+ channel subunits in adult rat heart. Relation to functional K^+ channels ? *Circ Res* **77:**361–369.

Brahmajothi MV, Morales MJ, Liu S, Rasmusson R, Campbell DL, and Strauss HC (1996) In situ hybridization reveals extensive diversity of K^+ channel mRNA in isolated ferret cardiac myocytes. *Circ Res* **78:**1083–1089.

Choi KL, Mossman C, Aube J, and Yellen G (1993) The internal quaternary ammonium receptor site of Shaker potassium channels. *Neuron* **10:**533–541.

Delgado C, Tamargo J, and Tejerina T (1985) Electrophysiological effects of propafenone in untreated and propafenone-pretreated guinea-pig atrial and ventricular muscle fibres. *Br J Pharmacol* **86:**765–775.

Dixon JE and McKinnon D (1994) Quantitative analysis of potassium channel mRNA expression in atrial and ventricular muscle of rats. *Circ Res* **75:**252–260.

Doyle DA, Cabral JM, Pfuetzner RA, Kuo A, Gulbis JM, Cohen SL, Chait BT, and MacKinnon R (1998) The structure of the potassium channel: molecular basis of K^+ conduction and selectivity. *Science (Wash DC)* **280:**69–77.

Duan D, Fermini B, and Nattel S (1993) Potassium channel blocking properties of propafenone in rabbit atrial myocytes. *J Pharmacol Exp Ther* **264:**1113–1123.

Dumont JN (1972) Oogenesis in *Xenopus laevis* (Daudin). I. Stages of oocyte development in laboratory maintained animals. *J Morphol* **136:**153–179.

Ficker E, Jarolimek W, Kiehn J, Baumann A, and Brown AM (1998) Molecular determinants of dofetilide block of HERG K^+ channels. *Circ Res* **82:**386–395.

Franqueza L, Longobardo M, Vicente J, Delpon E, Tamkun MM, Tamargo J, Snyders DJ, and Valenzuela C (1997) Molecular determinants of stereoselective bupivacaine block of hKv1.5 channels. *Circ Res* **81:**1053–1064.

Franqueza L, Valenzuela C, Delpon E, Lingobardo M, Caballero R, and Tamargo J (1998) Effects of propafenone and 5-hydroxy-propafenone on hKv1.5 channels. *Br J Pharmacol* **125:**969–978.

Hoppe UC and Beuckelmann DJ (1998) Modulation of the hyperpolarization-activated inward current (I_f) by antiarrhythmic agents in isolated human atrial myocytes. *Naunyn-Schmiedeberg's Arch Pharmacol* **358:**635–640.

Huang B, Qin D, and El-Sherif N (2000) Early down-regulation of K^+ channel genes and currents in the postinfarction heart. *J Cardiovasc Electrophysiol* **11:**1252–1261.

Johnson JW and Ascher P (1987) Glycine potentiates the NMDA response in cultured mouse brain neurons. *Nature (Lond)* **325:**529–531.

Kauder O, Madeja M, Speckmann E-J, and Lehmenkühler A (1991) Changes of free intracellular NH_4 concentration and cytosolic pH in the *Xenopus* oocyte during exposure to NH_4Cl. *Pfleugers Arch Eur J Physiol* **418**(Suppl 1)**:**R77.

Kohlhardt M (1984) Block of sodium currents by antiarrhythmic agents: analysis of the electrophysiologic effects of propafenone in heart muscle. *Am J Cardiol* **54:** 13D–19D.

Kobertz WR, Williams C, and Miller C (2000) Hanging gondola structure of the T1 domain in a voltage-gated K^+ channel. *Biochemistry* **39:**10347–10352.

Ledda F, Mantelli L, Manzini S, Amerini S, and Mugelli AJ (1981) Electrophysiological and antiarrhythmic properties of propafenone in isolated cardiac preparations. *Cardiovasc Pharmacol* **3:**1162–1173.

Liman ER, Tytgat J, and Hess P (1992) Subunit stoichiometry of mammalian K channel determined by construction of multimeric cDNAs. *Neuron* **9:**861–871.

Madeja M, Musshoff U, and Speckmann E-J (1991) A concentration-clamp system allowing two-electrode voltage-clamp investigations in oocytes of *Xenopus laevis*. *J Neurosci Meth* **38:**267–269.

Madeja M, Musshoff U, and Speckmann E-J (1997) Follicular tissues reduce drug effects on ion channels in oocytes of *Xenopus laevis*. *Eur J Neurosci* **9:**599–604.

Mergenthaler J, Haverkamp W, Hüttenhofer A, Skryabin BV, Mußhoff U, Borggrefe M, Speckmann E-J, Breithardt G, and Madeja M (2001) Blocking effect of the antiarrhythmic drug propafenone on the HERG potassium channel. *Naunyn-Schmiedeberg's Arch Pharmacol* **363:**472–480.

Methfessel C, Witzemann V, Takahashi T, Mishina M, Numa S, and Sakmann B (1986) Patch clamp measurements on *Xenopus laevis* oocytes: currents through endogenous channels and impantated acetylcholine receptor and sodium channels. *Pfleugers Arch Eur J Physiol* **407:**577–588.

Mitcheson JS, Chen J, Lin M, Culberson C, and Sanguinetti C (2000) A structural basis for drug-induced long QT syndrome. *Proc Natl Acad Sci USA* **97:**12329–12333.

Nishiyama A, Kambe F, Kamiya K, Seo H, and Toyama J (1998) Effects of thyroid status on expression of voltage-gated potassium channels in rat left ventricle. *Cardiovasc Res* **40:**343–351.

Qin D, Huang B, Deng L, El-Adawi H, Ganguly K, Sowers JR, and El-Sherif N (2001) Downregulation of K^+ channel genes expression in type I diabetic cardiomyopathy. *Biochem Biophys Res Commun* **283:**549–553.

Rolf S, Haverkamp W, Borggrefe M, Musshoff U, Eckardt L, Mergenthaler J, Snyders DJ, Pongs O, Speckmann E-J, Breithardt G, et al. (2000) Effects of antiarrhythmic drugs on cloned cardiac voltage-gated potassium channels expressed in *Xenopus* oocytes. *Naunyn-Schmiedeberg's Arch Pharmacol* **362:**22–31.

Satoh H and Hashimoto K (1984) Effect of propafenone on the membrane currents of rabbit sino-atrial node cells. *Eur J Pharmacol* **99:**185–191.

Schultz J-H, Volk T, and Ehmke H (2001) Heterogeneity of Kv2.1 mRNA expression and delayed rectifier current in single isolated myocytes from rat left ventricle. *Circ Res* **88:**483–490.

Singh BN (1997) Controlling cardiac arrhythmias: an overview with a historical perspective. *Am J Cardiol* **80:**4G–15G.

Snyders DJ (1999) Structure and function of cardiac potassium channels. *Cardiovasc Res* **42:**377–390.

Snyders DJ, Knoth KM, Roberds SL, and Tamkun MM (1992) Time-, voltage-, and state-dependent block by quinidine of a cloned human cardiac potassium channel. *Mol Pharmacol* **41:**322–330.

Valenzuela C, Delpon E, Tamkun MM, Tamargo J, and Snyders DJ (1995) Stereoselective block of a human cardiac potassium channel (Kv1.5) by bupivacaine enantiomers. *Biophys J* **69:**418–427.

Walsh KB, Sweet JK, Parks GE, and Long KJ (2001) Modulation of outward potassium currents in aligned cultures of neonatal rat ventricular myocytes during phorbol ester-induced hypertrophy. *Mol Cell Cardiol* **33:**1233–1247.

Xu H, Barry DM, Li H, Brunet S, Guo W, and Nerbonne JM (1999) Attenuation of the slow component of delayed rectification, action potential prolongation and triggered activity in mice expressing a dominant-negative Kv2 α subunit. *Circ Res* **85:**623–633.

Yellen G, Jurman ME, Abramson T, and MacKinnon R (1991) Mutations affecting internal TEA blockade identify the probable pore-forming region of a K^+ channel. *Science (Wash DC)* **251:**939–942.

Yeola SW, Rich TC, Uebele VN, Tamkun MM, and Snyders DJ (1996) Molecular analysis of a binding site for quinidine in a human cardiac delayed rectifier K^+ channel. *Circ Res* **78:**1105–1114.

Zhang S, Zhou Z, Gong Q, Makielski JC, and January CT (1999) Mechanism of block and identification of the verapamil binding domain to HERG potassium channels. *Circ Res* **84:**989–998.

Zhou M, Morais-Cabral JH, Mann S, and MacKinnon R (2001) Potassium channel receptor site for the inactivation gate and quaternary amine inhibitors. *Nature (Lond)* **411:**657–661.

Zhu X-R, Netzer R, Böhlke K, Liu Q, and Pongs O (1999) Structural and functional characterization of Kv6.2, a new γ-subunit of voltage-gated potassium channel. *Recept Channels* **6:**337–350.

Address correspondence to: Prof. Dr. Michael Madeja Hertie Foundation Department Neurosciences Lyoner Str. 15 D-60528 Frankfurt, Germany. E-mail: madejam@ghst.de